Investigation of magnetic structure and magnetization process of yttrium iron garnet film by Lorentz microscopy and electron holography

W. X. Xia,[1,a)] Y. S. Chun,[2] S. Aizawa,[1] K. Yanagisawa,[1,3] Kannan. M. Krishnan,[2] D. Shindo,[1,4] and A. Tonomura[1,3,5]
[1]*Advanced Science Institute, RIKEN, (c/o Advanced Research Laboratory, Hitachi, Ltd.), Hatoyama, Saitama 350-0395, Japan*
[2]*Department of Materials Science and Engineering, University of Washington, Seattle, Washington 98195, USA*
[3]*Okinawa Institute of Science and Technology, Kunigami, Okinawa 904-0411, Japan*
[4]*Institute of Multidisciplinary Research for Advanced Materials, Tohoku University, Sendai 980-8577, Japan*
[5]*Advanced Research Laboratory, Hitachi, Ltd., Hatoyama, Saitama 350-0395, Japan*

(Received 28 July 2010; accepted 29 October 2010; published online 30 December 2010)

The micromagnetic structure and magnetization process of perpendicular $Y_3Fe_5O_{12}$ (YIG) films were studied by Lorentz microscopy and electron holography. The closure domain structure inside the thin transmission electron microscopy specimen exhibits the same period as the magnetization pattern observed by magnetic force microscopy indicating the perpendicular anisotropy of the YIG film. Through observation of stray fields, it is concluded that the shapes of domain and domain walls are sensitive to the specimen thickness; moreover, a closure domain configuration observed in thin specimen is the stable energy state as determined by the balance between the crystalline anisotropy and shape anisotropy. Domain wall movement is observed by applying a magnetic field, *in situ*, inside the microscope in both horizontal and perpendicular directions; the saturation fields observed are qualitatively in agreement with the results of the hysteresis loop. © *2010 American Institute of Physics*. [doi:10.1063/1.3524273]

I. INTRODUCTION

Garnets are widely used materials in optical disks and microwave devices.[1,2] In particular $Y_3Fe_5O_{12}$ (YIG) films deposited on gadolinium-gallium-garnet (GGG) substrates under appropriate growth conditions exhibit perpendicular magnetic anisotropy due to epitaxial growth because of the good lattice-match between GGG and YIG.[2,3] In the evaluation of the magnetic structure of YIG films, the structure of domains is routinely estimated by magnetic force microscopy (MFM) and interpreted in terms of magnetic parameters, such as magnetic anisotropy constant and saturation magnetization.[4–6] Since the MFM image is sensitive only to stray field gradients at film surfaces, in such imaging the magnetization configuration inside the film remains unresolved. However, it is important to understand the mechanism of perpendicular magnetization in epitaxial YIG films and correlate the direction of magnetization with the growth process. Magnetic imaging carried out with transmission electron microscopes (TEMs), especially Lorentz microscopy and electron holography,[7,8] offer a quantifiable alternative to imaging by photons or scanning probes.[9] In this paper, the domain structure of YIG films, including its variation as a function of TEM specimen thickness t_s, was evaluated by Lorentz microscopy and electron holography. The specimens were magnetized *in situ* by applying a magnetic field inside the TEM in both horizontal and perpendicular directions. It is shown that the demagnetization field of the perpendicularly magnetized film plays an important role in determining the structure of domains and domain walls as well as the distribution of magnetic flux densities in the magnetization process.

II. EXPERIMENTAL PROCEDURE

The YIG films were deposited on GGG substrates by magnetron sputtering and its thickness t_f, ~0.89 μm, was optimized to maximize the perpendicular anisotropy.[2] The magnetic structure of samples was routinely imaged by MFM and the hysteresis loops were measured with a superconducting quantum interference device (SQUID). Electron transparent samples were then fabricated by focused ion beam (FIB) milling. Stray fields were observed by electron holography as a function of TEM specimen thickness, t_s, in the direction of incident electron beam. At $t_s \sim 0.11$ μm, domain walls were observed by Lorentz microscopy and the magnetic flux distributions were observed by electron holography using 300 kV Hitachi HF-3300X TEM, equipped with two electron biprism stages and an instrument for applying three dimensional magnetic fields *in situ*.[10] A voltage of 45 V was applied to the biprism and the interference fringe spacing was 6.1 nm for all observations.

III. RESULTS AND DISCUSSION

Figure 1 shows the MFM image of the YIG film. Strong periodic stripe contrasts are observed indicating perpendicular magnetization of the film. From the MFM images, the domains can be interpreted, to the first order, to be perpendicular to the film plane. In order to observe the domain structure in the interior of the YIG sample, thin film speci-

a)Electronic mail: xiawxing@riken.jp.

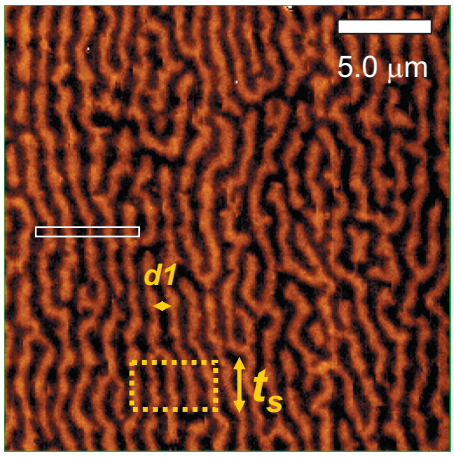

FIG. 1. (Color) MFM image of YIG film. White rectangle region is the position of TEM specimen in Fig. 2. Yellow dotted rectangle region with thickness t_s is the position of specimen in Fig. 3, and $d1$ is the domain width, ~0.5 μm.

mens for TEM observation were prepared by FIB in an area where the etching direction was normal to the stripe domains as shown by the white rectangle in Fig. 1. The corresponding TEM results are shown in Fig. 2, where (a) is the bright field image delineating the GGG-YIG interface and the PtPd surface layer used to avoid damage in the FIB etching process, and (b) and (c) are Lorentz images at overfocus and underfocus conditions, respectively. The poor contrast in Fig. 2(a) is due to the relatively thick TEM specimen, t_s=0.15 μm. Several TEM specimens with different thicknesses t_s were prepared and imaged; if the specimen was too thin the domain walls were not resolved except at extremely large defocused values with significantly distorted images. Note that a thick specimen (t_s>0.1 μm) for Lorentz imaging of YIG

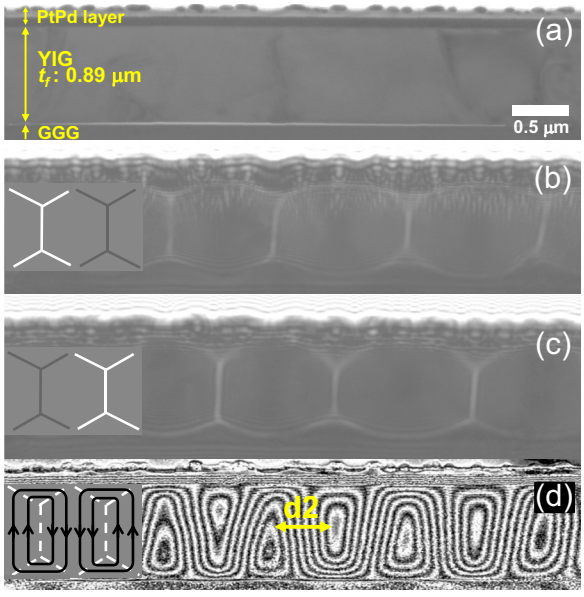

FIG. 2. (Color online) (a) Bright field image, (b) Lorentz micrographs for overfocus condition and (c) for underfocus condition, (d) holography image indicating the lines of magnetic flux. On the left-hand sides of (b) and (c), schematic diagrams are added to show domain walls with white and black lines; the corresponding lines of magnetic flux are depicted in (d), where $d2$ is the domain width, ~0.5 μm.

is required because of the low saturation magnetization, ~11 emu/cc. Figure 2 shows the thickest specimen (t_s =0.15 μm) for which both the domain walls at a low defocused value and the related electron hologram can be observed. Because Lorentz images are taken at the defocused states, domain walls of ferromagnetic materials can be observed in white or black contrast. Although the black contrasts for domain walls are not easily visible for this material, we can determine the black contrast positions by comparing a pair of Lorentz images taken at underfocus and overfocus conditions as shown in Figs. 2(b) and 2(c), respectively; the clear white contrasts in the overfocused condition in (b) become the black contrasts in the corresponding position in the underfocused condition (c), and vice versa. To indicate these correlations, schematic diagrams are depicted on the left-hand sides of (b) and (c). (Based on this argument, in other Lorentz images the black contrasts for domain walls are indicated by dashed lines). Note that the domain walls are straight at the central region of the film while they curve at both the top surface and the bottom interface to the substrate. Figure 2(d) is the reconstructed phase image with the phase amplification of 2.0 and the image is depicted by cosine function of phase shift. [The schematic diagram is shown on the left-hand side corresponding to the domain wall positions in (b) and (c)]. Periodic closure domains are now observed indicating the most energetically favorable state of the film. From the closure domain configuration shown in Fig. 2(d), we conclude that the film has perpendicular anisotropy but with a weak anisotropy field comparable to the demagnetization field in the perpendicular direction. On the other hand, if the perpendicular magnetic anisotropy were strong enough, the domain walls would remain normal throughout the entire film thickness t_f, and the magnetic flux will close through stray fields outside the film. The period of the closure domains $d2$ in Fig. 2(d), is determined by the balance between perpendicular anisotropy and demagnetization energy as well as the domain wall energy. This period, ~0.5 μm, corresponds to the distance between the centers of a couple of "black" and "white" domain walls in the in-focus state. Although this period is in agreement with that estimated from the MFM image, the domain structures in Fig. 2 disagree with those of the stray fields observed by MFM. Specifically, the domain structures observed in Fig. 2(b) or Fig. 2(c) do not produce any stray fields and therefore the MFM images would show no contrast. It is plausible, however, that the domain structures observed by MFM in the original thin films were subsequently altered during the preparation of the electron transparent TEM specimen.

In order to probe changes in the domain structure, we decreased t_s of TEM specimen, in the direction of the electron beam and observed its stray field distribution. An equivalent area with a uniform stripe domain, indicated by the yellow dashed rectangle in Fig. 1, was selected and gradually etched with FIB to reduce its thickness t_s. Figure 3 shows stray field distributions for (a) t_s=4.38 μm, (b) t_s =3.20 μm, and (c) t_s=1.88 μm, where the phase amplification coefficients are set at 8. Figure 3(d) shows simultaneously the magnetic flux inside and the stray fields outside of the same TEM specimen (t_s=0.11 μm). The amplification

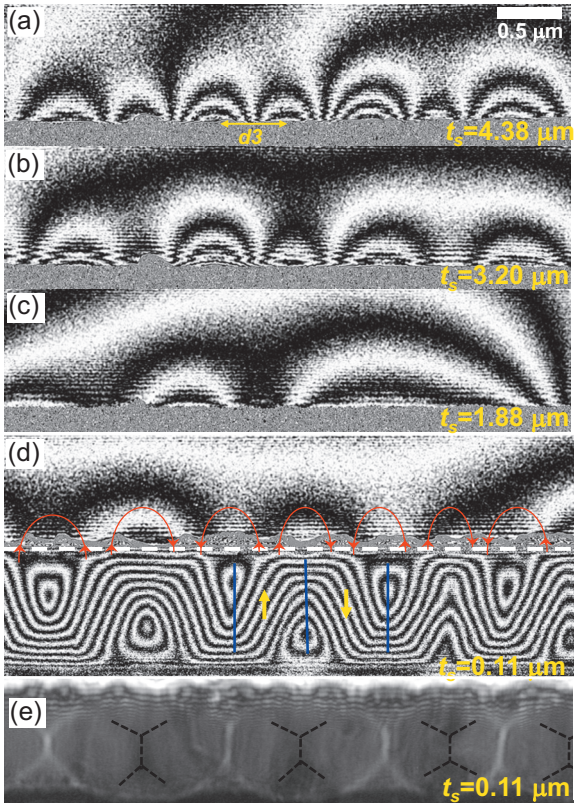

FIG. 3. (Color) (a)–(c) are holography images of stray magnetic fields outside the specimen for the specimen thickness t_s of 4.38 μm, 3.20 μm, 1.88 μm, respectively. (d) is the stray magnetic fields outside the specimen and the magnetic flux inside the thin specimen with thickness of 0.11 μm. (e) is the underfocus image of (d) showing the domain walls in white contrast, where the black contrasts for domain walls are emphasized by dashed lines.

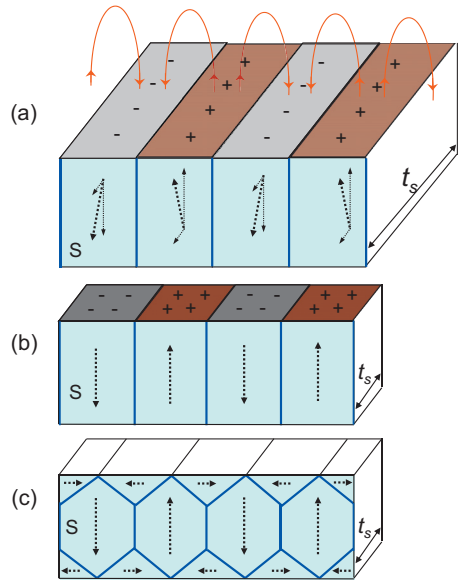

FIG. 4. (Color) Schematic diagram of changes in domain structures and domain walls with decreasing the specimen thickness t_s. Blue solid lines represent domain walls and dashed black arrows represent the magnetization direction in each domain. + and − represent the positive and negative surface charges, respectively. In (a), t_s is large and red curves represent stray fields. (b) and (c) are the cases of laminated and closure domain structures with small t_s, respectively.

coefficient for stray fields is set at 8 to compare it with those in Figs. 3(a)–3(c), whereas the amplification coefficient for phase inside the specimen is set at 2. The stray fields in Fig. 3(a) are periodic. When t_s is decreased to 3.20 μm, Fig. 3(b), the period stays the same while only the strength becomes weak. The domain width measured from the stray field period $d3$, shown in Fig. 3(a), is approximately 0.5 μm. However, when t_s reached 1.88 μm in (c) and less (not shown in the figure), the periodicity of the stray fields are destroyed. When t_s becomes 0.11 μm in Fig. 3(d), no regular stray field patterns can be observed because most magnetic fluxes are close inside the specimen. Figure 3(e) shows the domain images at the underfocus Lorentz condition, where the black contrasts for domain walls are indicated by dashed lines. Let us discuss domain wall structures in Fig. 3(d) in more detail. If in an as-grown YIG film, domain walls are straight as shown by the blue lines and magnetization directions are completely perpendicular to the thin film plane as shown by the yellow arrows, stray fields will be generated as shown by the red curves above the specimen surface which is in good agreement with the observed stray field pattern in Fig. 3(a). Therefore, it is suggested that the original domain walls become curved in the top surface region and the bottom YIG-GGG interface region when the specimen thickness t_s is decreased. Possible reasons for this curvature are a change in the demagnetization field along t_f [the thickness of YIG film in Fig. 2(a)] and an influence of damage layers produced by FIB etching. However, the balance between the demagnetization field and anisotropy field along t_f does not depend on the specimen thickness t_s, and moreover, the damage layers introduced by FIB are very thin (~0.01 μm) compared to t_s, (~2.0 μm) at which the stray fields begin to deform.

A more reasonable interpretation is schematically shown in Fig. 4 based on the argument on stripe domain structures related to rotatable magnetic anisotropy.[11–13] In the as-grown film or thick TEM specimen with large t_s [Fig. 4(a)], the magnetization has both perpendicular and horizontal components and the stripe domains in Fig. 1 appear when the perpendicular anisotropy is not greater than the demagnetization field; the perpendicular anisotropy is considered to be induced by growth process in which the preferential sites are occupied by rare-earth atoms in the garnet lattice.[3,4] The stripe period or the domain width is determined by the saturation magnetization, exchange stiffness constant, and film thickness. The perpendicular components of magnetization result in magnetic charges as indicated by "+" and "−" and stray fields as indicated by red curves in Fig. 4(a). On the other hand, the horizontal components of magnetization will result in magnetic charges at the TEM specimen surface, S (indicated in light blue in the figure and the opposite surface). When t_s is large, the effect of the magnetic charges in the surface S and the opposite surface can be ignored and the domain walls are straight as shown by blue lines, as anticipated from Fig. 3. When t_s is decreased, the effect of the charges at the surfaces S and the opposite surface will become large and the energy state in Fig. 4(a) is destroyed. As a result, the in-plane components (perpendicular direction in as-grown film) shown in Figs. 4(b) and 4(c) become larger

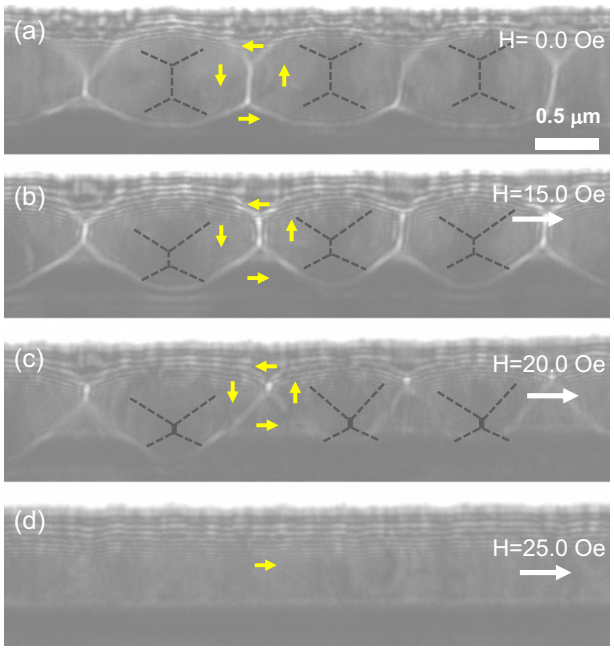

FIG. 5. (Color online) *In situ* observation of magnetization process in Lorentz imaging when applying horizontal magnetic field indicated by white arrows. (a) is for zero magnetic field. (b)–(d) show domain walls for 15.0 Oe, 20.0 Oe, and 25.0 Oe, respectively. White lines indicate domain walls in underfocus Lorentz conditions. Black dashed lines are used to emphasize domain walls in black contrasts. Arrows in the middle indicate the magnetization direction of domains.

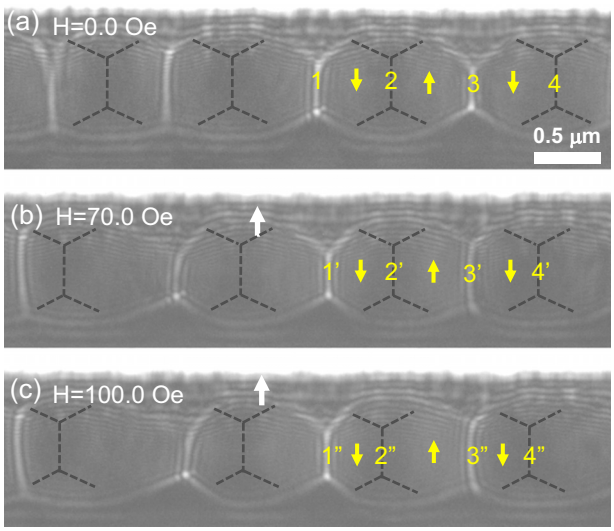

FIG. 6. (Color online) *In situ* observation of magnetization process in Lorentz imaging when applying perpendicular magnetic fields indicated by white arrows for, (a) 0.0, (b) 70.0, and (c) 100.0 Oe. Black dashed lines indicate domain walls in black contrasts. The numbers indicate examples of domain-wall positions and arrows near the numbers indicate magnetization directions of domains.

than those shown in Fig. 4(a). [In Figs. 4(b) and 4(c), the remaining small out-of-plane components are not shown for brevity. In Fig. 4(b) the increased surface charge densities are indicated in darker colors with + and − signs]. Two domain structures can be formed for materials with different intrinsic magnetic properties: laminated domains with charges in the upper and lower surfaces shown in Fig. 4(b) and closure domains with no charges at those surfaces shown in Fig. 4(c). Generally, laminated domains appear under high uniaxial anisotropy conditions and closure domains appear under low cubic anisotropy conditions. As exhibited in the observation results in Figs. 2 and 3, closure domain structure is energetically favorable for the present garnet with the cubic crystalline anisotropy.

Next we carried out *in situ* experiments by applying a magnetic field to thin specimens to observe changes in domain structures during the magnetization process. The magnetic fields are applied in both horizontal and perpendicular directions with respect to the TEM specimen. Figure 5 shows the horizontal results, in which we focus on one domain wall and indicate the magnetization direction of domains by yellow arrows. The magnetic field H was applied from 0 to 25.0 Oe in steps of 5.0 Oe. There are no distinct changes when $H<10.0$ Oe, whereas when $H=15.0$ Oe [Fig. 5(b)], the straight domain walls at the center of the specimen moved upwards; as a result, the region of magnetization parallel to the applied field (lower section) increased. At the same time, the region with magnetization direction antiparallel to the applied field (upper section) decreased. When $H=20.0$ Oe, the straight domain walls became almost spots and moved further upwards (simultaneously the dark spots moved downwards, which was more clearly shown in overfocus images), and the area of the lower part was further enlarged and the upper part reduced. However, the domain period remained unchanged in this process. When $H=25.0$ Oe, all domain walls disappeared and the film was uniformly magnetized in the direction of the applied field.

Figure 6 shows the magnetization process for the perpendicular magnetic field condition. Figure 6(a) shows $H=0.0$ Oe state where four domain walls are marked by 1, 2, 3, and 4; the magnetization directions of the domain are indicated by yellow arrows. The magnetic field was increased from 0.0 to 100.0 Oe in steps of 10.0 Oe. Unlike the horizontal magnetic field results (Fig. 5), no observable changes in domains appeared when $H<50.0$ Oe. Figures 6(b) and 6(c) show the domain structures when $H=70.0$ Oe and 100.0 Oe, respectively. The domain walls shifted horizontally with increasing magnetic field. The domain walls 1′, 2′, 3′, and 4′ in Fig. 6(b) and 1″, 2″, 3″, and 4″ in Fig. 6(c) indicate new positions of the domain walls 1, 2, 3, and 4 in Fig. 6(a). To minimize the Zeeman energy, domains with the magnetization direction along the applied field, for example the domain between 2 and 3 grew and domains with the magnetization direction antiparallel to the magnetic field, for examples the domain between 1 and 2 decreased. These *in situ* experimental results indicate that magnetization in horizontal direction of the TEM specimen are more easily saturated than those in perpendicular direction. We measured the hysteresis loop of the as-grown YIG films by SQUID in both horizontal and perpendicular directions and found out that the saturation fields in the horizontal and perpendicular directions were 100 Oe and 800 Oe, respectively; this is qualitatively in agreement with the *in situ* TEM observation results.

IV. CONCLUSION

The period of the closure magnetic domains in thin YIG specimens, evaluated by Lorentz microscopy and electron

holography, agreed with the surface magnetization pattern observed by MFM. It was confirmed that the magnetic domain structure changed due to the demagnetization field when the TEM specimen was thinned. *In situ* observation exhibited the easy horizontal magnetization direction of YIG film. The results presented in this paper are helpful for optimizing the magnetic anisotropy of YIG in fabrication process and understanding its magnetization process.

ACKNOWLEDGMENTS

The works of W. X. Xia, S. Aizawa, K. Yanagisawa, and A. Tonomura were supported by the Funding program for world-leading Innovative Research and development on Science and Technology by Japanese Government. The work at the University of Washington was supported by the U.S. Department of Energy under Grant No. BES-ER45987.

[1]Q. H. Yang, H. W. Zhang, Q. Y. Wen, Y. L. Liu, and J. Q. Xiao, J. Appl. Phys. **105**, 07A501 (2009).
[2]Y. S. Chun, H. Ohldag, and K. M. Krishnan, IEEE Trans. Magn. **43**, 3004 (2007).
[3]K. M. Krishnan, A. B. Pakhomov, Y. Bao, P. Blomqvist, Y. Chun, M. Gonzales, K. Griffin, X. Ji, and B. K. Roberts, J. Mater. Sci. **41**, 793 (2006).
[4]Y. Shimada, J. Appl. Phys. **45**, 4598 (1974).
[5]M. Pardavi-Horvath, IEEE Trans. Magn. **21**, 1694 (1985).
[6]K. M. Krishnan, P. Rez, and G. Thomas, Acta Crystallogr., Sect. B: Struct. Sci. **41**, 396 (1985).
[7]D. Shindo, Y. G. Park, Y. Gao, and H. S. Park, J. Appl. Phys. **95**, 6521 (2004).
[8]A. Tonomura, *Electron Holography*, 2nd ed. (Springer, New York, 1999), p. 85.
[9]G. Srajer, L. H. Lewis, S. D. Bader, A. J. Epstein, C. S. Fadley, E. E. Fullerton, A. Hoffmann, J. B. Kortright, K. M. Krishnan, S. A. Majetich, T. S. Rahman, C. A. Ross, M. B. Salamon, I. K. Schuller, T. C. Schulthess, and J. Z. Sun, J. Magn. Magn. Mater. **307**, 1 (2006).
[10]J. J. Kim, K. Hirata, Y. Ishida, D. Shindo, M. Takahashi, and A. Tonomura, Appl. Phys. Lett. **92**, 162501 (2008).
[11]R. J. Spain, Appl. Phys. Lett. **3**, 208 (1963).
[12]N. Saito, H. Fujiwara, and Y. Sugita, J. Phys. Soc. Jpn. **19**, 1116 (1964).
[13]S. Chikazumi, *Physics of Ferromagnetism* (Oxford Science, New York, 1996), p. 336.